A Numerical Investigation of Phase-Locked and Chaotic Behavior of Coupled van der Pol Oscillators

Lesley Ann Low, Per G. Reinhall and Duane W. Storti
Department of Mechanical Engineering
University of Washington
Seattle, Washington 98195 USA

July 11, 2000

Abstract

Limit cycle oscillators arise in a wide variety of mechanical, electrical and biological systems. Recently, emphasis has been placed on the study of systems of coupled limit cycles, such as cardiac oscillations. Synchronization criteria have remained a focus of most investigations.

One area of investigation in the field of coupled limit cycles is studying the behavior of a pair of linearly coupled van der Pol oscillators [32, 46, 50]. Previous investigations [57, 58] found the stability regions of the coupled oscillators for their in-phase and out-of-phase modes numerically.

This research presents results obtained from numerical analysis of a pair of coupled van der Pol oscillators describing new dynamic behavior; phase-locked trajectories and non-periodic behavior. Also presented are the stability regions and a description of new dynamic behavior of a pair of coupled van der Pol oscillators with detuning.

1 INTRODUCTION

Limit cycle oscillators arise in many biological, mechanical and electrical systems such as fireflies that flash in unison, large groups of crickets that synchronously chirp [16], cell division [39], pacemaker cells in the heart, the neural networks in the spine and brain that control rhythmic actions such as breathing and chewing [16], electric circuits with nonlinear resistance [57], vibrations of bluff bodies in a crossflow [7], predator-prey interactions [31] and stomatal oscillations [47]. It is because of the remarkable efficiency of these oscillators that the dynamic behavior of limit cycle oscillators has been studied in great depth.

The van der Pol equation has been adopted as a common mathematical model for limit cycle oscillators [57] and has been the subject of numerous studies and its behavior is well understood. The governing equation for the van der Pol oscillator is:

$$\ddot{x} + \varepsilon(x^2 - 1)\dot{x} + x = 0 \tag{1}$$

where the dot represents differentiation with respect to time. The van der Pol oscillator has self-sustained oscillations due to the non-linear damping term $(x^2 - 1)\dot{x}$. When $|x| < 1$, the damping term has a negative value making the system absorb energy. When $|x| > 1$, the damping term has a positive value, meaning the system dissipates energy [4, 23]. The van der Pol oscillator will reach a steady state oscillation with constant amplitude independent of initial conditions. This isolated, periodic oscillation is called a limit cycle. A limit cycle is represented in the phase plane by an isolated closed-loop path.

The non-linearity parameter, ε, affects the damping of the oscillator, which greatly affects the solution of the van der Pol equation. When $\varepsilon \ll 1$ the solution of the van der Pol equation is approximately $x(t) = 2\cos(t) + O(\varepsilon)$. When $\varepsilon \gg 1$ the oscillator is nonsinusoidal displaying the behavior of a relaxation oscillator which has periodic behavior characterized by a low build up followed by a sudden discharge [23].

Relaxation oscillators occur in physical phenomenon such as: the beating of a heart [63], clock ticking [34], and stick-slip motion of a solid sliding across a rough surface [48]. Belair presents these and other examples in detail [6].

Numerous investigations have been conducted for many years studying varying aspects of the van der Pol oscillator. Focusing on a single van der Pol oscillator, some research has investigated the period and frequency [3], bifurcation of a limit cycle [25], chaos [51] and relaxation oscillations [22]. The natural course of the analysis of the van der Pol equation led to studying the response to periodic external forcing with attention focusing on questions of synchronization, frequency locking and phase entrainment [17, 19, 20, 21, 62].

Recently, research has shifted towards the study of the behavior of a system of coupled oscillators, with the main focus on synchronization criteria. The behavior of a pair of coupled limit cycle oscillators display a much wider range of phenomenon than a single limit cycle oscillator and can be used to model many different systems, such as cardiac cells [39], gas flux control in plant leaves, vibrations of heat exchanger tube banks, Raleigh-Benard convection cell dynamics

and neural synapses of a swimming fish [12].

Rand and Holmes first formulated and studied the problem of a pair of van der Pol oscillators with weak linear diffusive coupling. The governing equations are written as:

$$\begin{aligned} \ddot{x} + \varepsilon(x^2 - 1)\dot{x} + x &= \varepsilon A(y - x) + \varepsilon B(\dot{y} - \dot{x}) \\ \ddot{y} + \varepsilon(y^2 - 1)\dot{y} + (1 + \varepsilon\Delta)y &= \varepsilon A(x - y) + \varepsilon B(\dot{x} - \dot{y}) \end{aligned} \tag{2}$$

where x and y are the dependent variables, A and B are the coupling parameters, ε is the non-linearity parameter and Δ represents the detuning.

When viewing these equations as a mechanical system, x and y could be interpreted as the displacements of the masses with εA and εB as an attached spring and damper connecting the two masses. The detuning parameter, Δ, allows for the natural frequency of one oscillator to vary from the natural frequency of the other oscillator by introducing a small difference, $\varepsilon\Delta$, in the spring coefficient [48]. The coupling is weak since the O(ε) coupling terms are small for $\varepsilon \ll 1$ and diffusive so that if two cells that oscillate independently were placed next to each other the solutes would flow between them via diffusion and the coupling would be in terms of the concentration differences, (x - y) and ($\dot{x}$ - $\dot{y}$) [46, 57].

When the coupling terms are equal to zero (with zero or weak detuning), the system consists of two oscillators each evolving on a limit cycle that is orbitally stable in a 2-dimensional phase space, independent of the phase relationship. With nontrivial coupling, the oscillators interact resulting in trajectories perturbed from the uncoupled limit cycles embedded in the new 4-dimensional phase space that can be written as:

$$X = R_1(t)cos(t - \theta_1(t)), \quad Y = R_2(t)cos(t - \theta_2(t)) \tag{3}$$

where R_i(t) represents amplitude modulation and θ_i represents frequency modulation of a near limit cycle solution [9, 25]. The periodic phase-locked motions are characterized by constant values of the amplitudes, R_1 and R_2, and the phase difference, $\phi = \theta_1$ - θ_2.

Many studies have been conducted on various aspects of the pair of coupled oscillators using different techniques. Rand and Holmes [46] used the two variable method [27, 41] to determine the periodic solutions and their stability of the pair of coupled oscillators. Storti and Rand [55] studied the dynamics of strongly coupled oscillators with displacement coupling (B = 0) in the sinusoidal limit ($\varepsilon = 1$). The transition of the coupled oscillators from phase-locked motion (phase lag is fixed) to phase entrainment (phase lag varies periodically with a fixed mean) to drift (phase lag grows without bound) as detuning increases in weak displacement coupling (B = 0) was presented by Chakraborty and Rand [9]. In the relaxation limit ($\varepsilon \gg 1$ for Eq. 2), Belair [5] studied velocity coupling in a related system with piece-wise linear damping. Storti and Rand [56] studied the coupled system with strong displacement coupling (B = 0) having no detuning ($\Delta = 0$) using a linear variational equation and Floquet analysis.

More recently, Storti et al. [54] and Storti and Reinhall [57] solved the variational equation developed by Storti and Rand [56] using an adapted high order perturbation expansion approach (used by Andersen and Geer [3] and Dadfar et al. [13]). This analysis lead to a complete set of transition curves for the in-phase and out-of-phase modes for displacement coupling (B = 0) and velocity coupling (A = 0). From this analysis the stability regions for the in-phase and out-of-phase modes in the (A, B, ε) space for B $\neq$ 0 and A $\neq$ 0 were completed [57].

This paper presents a numerical investigation of two coupled van der Pol oscillators. The stability of the in-phase mode as reported in [57, 58] is revisited and extended, new dynamic behavior is presented and the effect of the stability of the in-phase mode with increasing detuning in the system is presented.

2 Numerical Results

In order to extend the analytical results previously reported[57, 58] a numerical investigation of the stability of the in-phase mode was performed. The numerical study was aimed at investigating the affect of the diffusive coupling on a system of two van der Pol oscillators, therefore the detuning was initially set to zero. While investigating the in-phase mode stability new dynamic behavior was discovered such as two phase-locked motions and non-periodic (chaotic) behavior.

Of initial interest was the stability boundary representing the transition from in-phase stability to in-phase instability. Figure 1 shows the transition curve of the coupled van der Pol oscillators for $\varepsilon = 2.5$, where the x-axis is εA ('spring') and the y-axis is εB ('damper'). The important features of this graph include:

- The vertical line of εA = -0.5 represents the minimum value of displacement coupling for stability. To the left of this line, regardless of the velocity coupling εB, the in-phase mode is unstable. This line does not depend on ε and not only separates in-phase stability and instability but also separates oscillatory solutions from non-oscillatory solutions.

- The in-phase mode is stable in the region bounded by the transition graph on the bottom and the vertical line of εA = -0.5 to the left.

- The in-phase mode is unstable to the right of εA = -0.5 and below the curve.

- The out-of-phase mode is stable in the region bounded on top by the horizontal line εB = 0 and on the left by the vertical line of εA = -0.5. Therefore, both the in-phase mode and out-of-phase mode are stable in the region above the transition curve and below εB = 0.

- The horizontal line segments represent the B_{zmd}, zero mean damping. This value is the critical velocity coupling where the in-phase mode is unstable when the velocity coupling is below this value. The B_{zmd} line is negative and increases in magnitude as ε increases. As ε increases, the B_{zmd} line shifts 'down' the εB axis faster than the actual transition ovals. Therefore at large ε values the horizontal B_{zmd} line is not part of the transition curve. The value of B_{zmd} can be determined using higher order expansion in the equation: $B_{zmd} = -\frac{\varepsilon}{2}(u^2 - 1)$, where u is the limit cycle of the van der Pol equation as outlined in [3].

- The ovals or 'bumps' in the transition graph come from the coefficients of the Hill's equation. These coefficients give instability points for $\varepsilon = 0$ as shown in [58].

One note of interest in Figure 1 is that the curve goes above the εB = 0 line. This means that the in-phase mode is unstable with small positive coupling. This result can be counter-intuitive because of our knowledge of phase coupling.

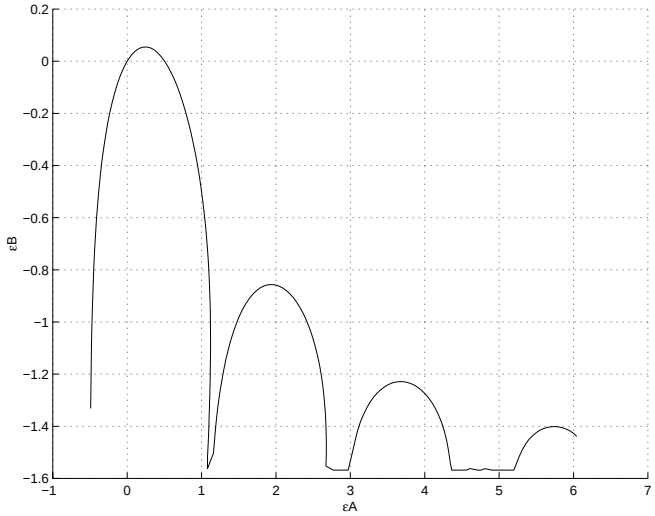

Figure 1: Transition Curve, $\varepsilon = 2.5$.

With zero detuning the coupled oscillators are identical, one would expect the positive damping would decrease a difference in velocity between the oscillators. Similarly a difference in amplitude would be expected to be decreased by a positive spring.

The findings from Storti and Reinhall [57, 58] and the numerical results show regions in the positive εA and εB plane where the in-phase mode is unstable. The reason for this non-intuitive result is that phase coupling is based on sinusoidal limit cycles. With $\varepsilon = 2.5$, the limit cycle of the van der Pol oscillator is not sinusoidal and as ε grows the limit cycle becomes even less sinusoidal and therefore less important in the determination of the stability regions of the coupled oscillators.

Figure 2 shows the transition curves for ε values of 0.5 through 10 in 0.5 increments. The uppermost line extending to the right of the graph represents the transition curve for $\varepsilon = 0.5$, the lowermost line represents the transition curve for $\varepsilon = 10$. The $\varepsilon = 0.5$ curve has the smallest oval on the left. As ε increases, the ovals grow in size and the B_{zmd} line extending across the εA values moves down (decreasing εB). As stated earlier, the B_{zmd} line moves down the εB axis faster than the ovals as ε grows. This can be seen by comparing the transition curve for $\varepsilon = 2$ and $\varepsilon = 10$. For $\varepsilon = 10$ the transition curve displays no horizontal line as the B_{zmd} line is found at εB = -8.166, far below the ovals.

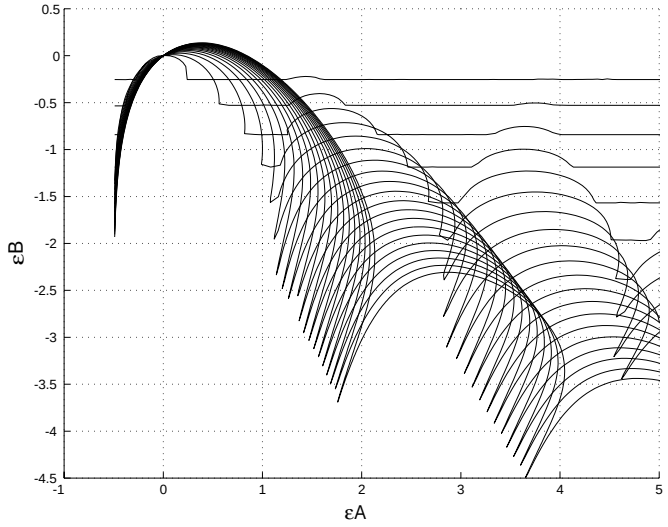

Figure 2: Transition Curves, $\varepsilon = 0.5{:}10$ in $\varepsilon = 0.5$ increments. ($\varepsilon = 0.5$ on top and $\varepsilon = 10$ on bottom.)

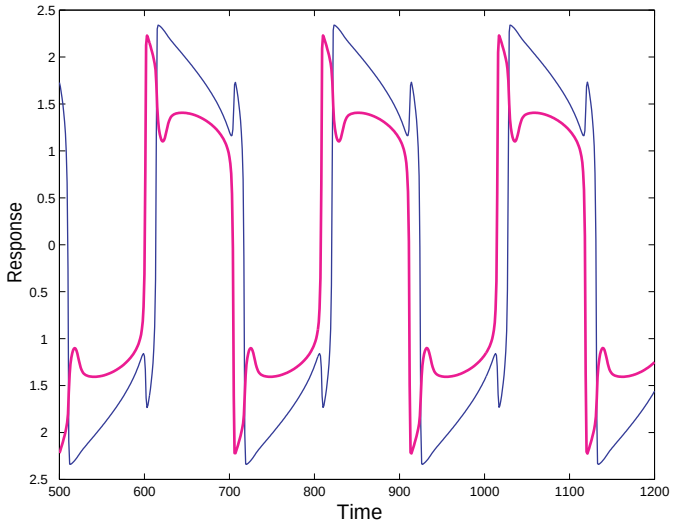

Figure 3: Shifted Asymmetric Trajectory (ε = 10, εB = -2.5, εA = 1.765).

3 Phase-Locked Trajectories

In addition to the in-phase and out-of-phase motion, we also found two shifted phase-locked motions. These shifted phase-locked motions occur when the oscillators are neither identical (in-phase) nor a reflection of each other (out-of-phase). Instead, the motion is characterized by each oscillator having a different zero-crossing time. The two phase-locked modes are shifted asymmetric mode and shifted symmetric mode.

The shifted asymmetric mode is defined by the zero crossings of each oscillator being a fixed time lag apart. Figure 3 shows a sample time history of the two oscillators locked in the shifted asymmetric mode (ε = 10, εB = -2.5, εA = 1.765). This time trace shows that the motion of the two oscillators is not the same. Minimally, the oscillators will have distinct amplitudes and quite often the motion of the oscillators (shape of response) will be distinct. Even with different amplitudes and shape, the concept of phase lag is still valid when the phase lag, ϕ, is defined in terms of the time lag, δt, and period, T, as shown in the following equation.

$$\phi = 360^o \frac{\delta t}{T} \tag{4}$$

The second shifted phase-locked mode, shifted symmetric, is characterized by one oscillator having zero crossings which alternate between being ahead and behind the other oscillator. Each oscillator has the same amplitude and the time trace of one oscillator is equal to half a period shift and a reflection of the other oscillator. Figure 4 shows a sample time history of the two oscillators locked in the shifted symmetric mode (ε = 10, εB = -2.5, εA = 2.75).

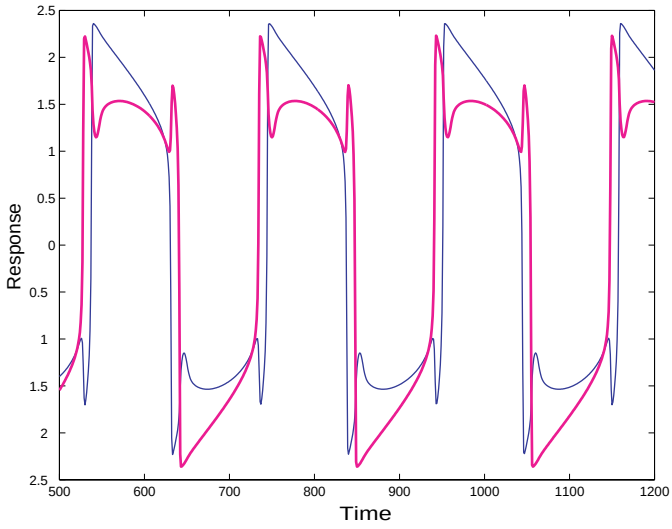

Figure 4: Shifted Symmetric Trajectory (ε = 10, εB = -2.5, εA = 2.75).

Figure 5 shows the transition curve for ε = 10, that includes the stability regions for the phase-locked modes. The larger left most region defines the region where the shifted asymmetric mode is found. In the smaller enclosed region defines the area where the shifted symmetric mode is found. These phase-locked areas remain in approximately the same locations as epsilon changes. Figure 6 shows the transition curves for ε = 10, 7.5, 5 and 2.5, respectively, each with the shifted asymmetric and shifted symmetric regions included. Both the shifted phase-locked motions are found to disappear for $\varepsilon < 2.5$.

Figure 7 shows how the phase lag, ϕ, changes from the in-phase stability region through the shifted asymmetric region into the in-phase unstable region as εB changes with εA = 0.3 and ε = 10.0. The phase angle remains at 0^o until εB = 0.125 when the oscillators cross the transition curve and enter the shifted asymmetric region. The oscillators remain in the shifted asymmetric region until εB = -0.2, where they move into the in-phase unstable region where the phase angle jumps to 180^o.

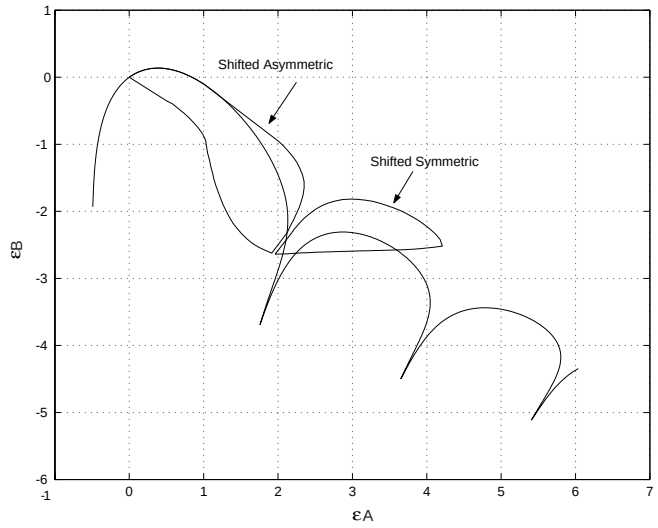

Figure 5: Transition Curve, $\varepsilon = 10$, with Shifted Symmetric and Shifted Asymmetric Regions.

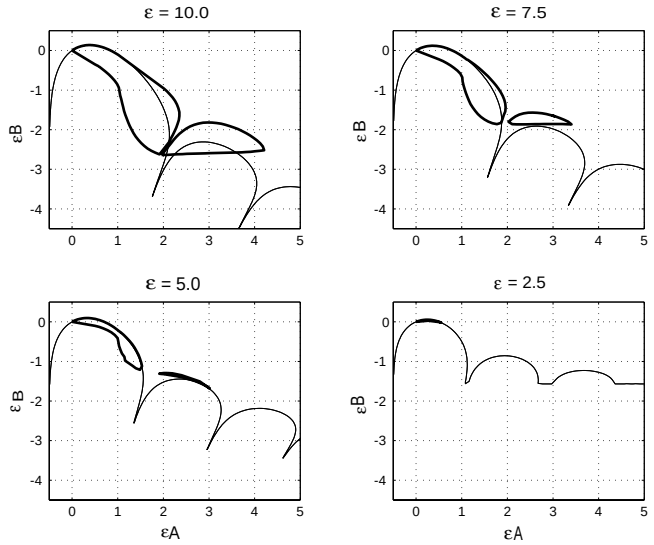

Figure 6: Transition Curve, $\varepsilon = 10.0$ (Upper Left), 7.5 (Upper Right), 5.0 (Lower Left), 2.5 (Lower Right) with Shifted Symmetric and Shifted Asymmetric Regions.

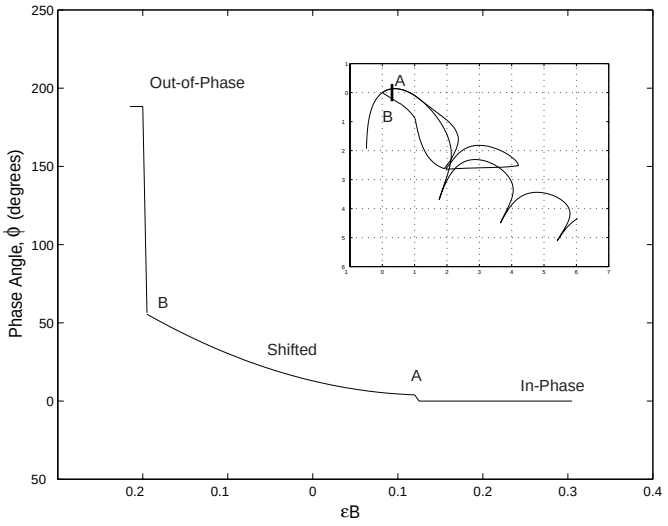

Figure 7: Phase Lag (ϕ) vs. εB ($\varepsilon = 10$, εA $= 0.3$).

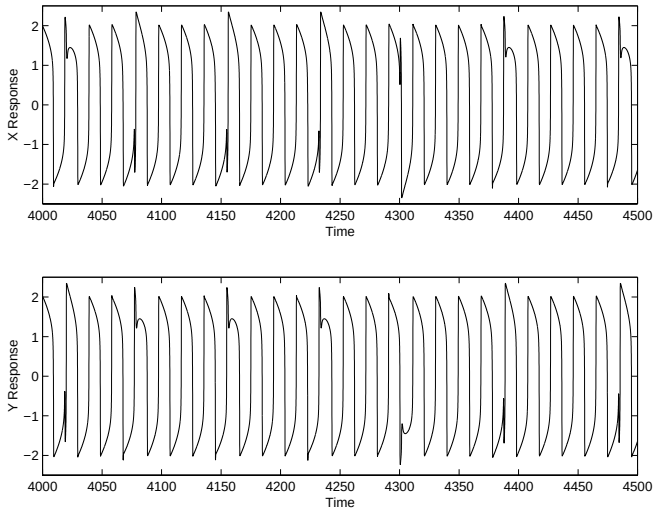

Figure 8: Time History of Chaotic Regime (ε = 10, εB = -2.5, εA = 2.033).

4 Non-Periodic Behavior

A small region of chaotic motion was also found below the transition curve and between the two phase-locking regions. For ε = 10 this region is a thin strip extending from approximately εA = 1.95 and εB = -2.6 on the lower left to εA = 2.08 and εB = -2.4 on the upper right.

Figure 8 shows a time history of the chaotic response at ε = 10, εB = -2.5, εA = 2.033. Figure 9 shows the corresponding strange attractor in the x, y, $\frac{dx}{dt}$ space.

The bifurcation map of Figure 10 shows the maximum peak of the response of the x oscillator as εA is changed along a path connecting the two shifted phase-locked responses. The line at approximately 2.35 corresponds to the amplitude of the out-of-phase mode which is also stable at this part of the parameter space.

The location of the chaotic region is below the transition curve (where the in-phase mode is unstable) and between the shifted symmetric and shifted asymmetric regions regardless of the ε value. As ε grows, the shifted regions grow larger and are located farther underneath the transition curve, as shown by Figures 5 and 6. Therefore the chaotic region grows in 'height' (εB). Figure 11 shows the transition curves with the chaotic regions for selected ε values (ε = 8.5, 9.5, 10, 10.5, 11.5 and 12.5). The chaotic region is represented by the dark marks on the graphs. This region is generally found on the right hand side of the left most oval, near where the two ovals come together. The figure for the non-linear parameter ε = 10 (center left) also shows the phase locked regions. Figure 11 shows the chaotic region, barely visible at ε = 8.5, growing as the non-linear parameter grows. It is clear to see that the chaotic behavior is found below the transition curve where the in-phase mode is unstable and

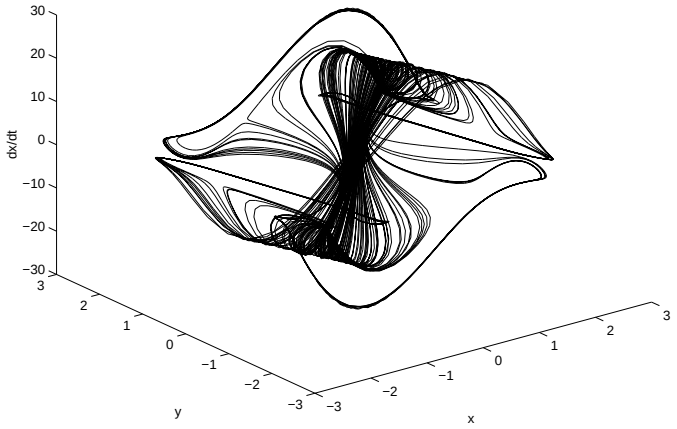

Figure 9: Phase Space Plot (ε = 10, εB = -2.5, εA = 2.033).

between the two shifted regions.

As stated earlier, chaos is found below the transition curve and between the shifted phase-locked regions. Therefore, at small ε values where the shifted phase-locked regions either disappear ($\varepsilon = 2.5$) or shrink sufficiently so that they are no longer in line with each other and the space between them is not found below the transition curve ($\varepsilon = 5.0$) the region where the chaotic behavior is found is eliminated. This can be seen from Figure 6. The smallest ε value where chaotic behavior is found is $\varepsilon = 7.5$. Here the space between the shifted asymmetric and shifted symmetric regions is found below the transition curve in a very small area. Thus, the chaotic behavior for $\varepsilon = 7.5$ is found in a much smaller region than higher ε values. As ε grows from 7.5 the chaotic region grows in terms of both the coupling parameters (εA and εB). At large ε values ($\varepsilon \geq 17$) the shifted regions continue to grow and nearly come together under the transition curve thus almost completely eliminating the chaotic region. At these large ε values, the size of the chaotic region is very small, on the same scale as the chaotic region for $\varepsilon = 7.5$.

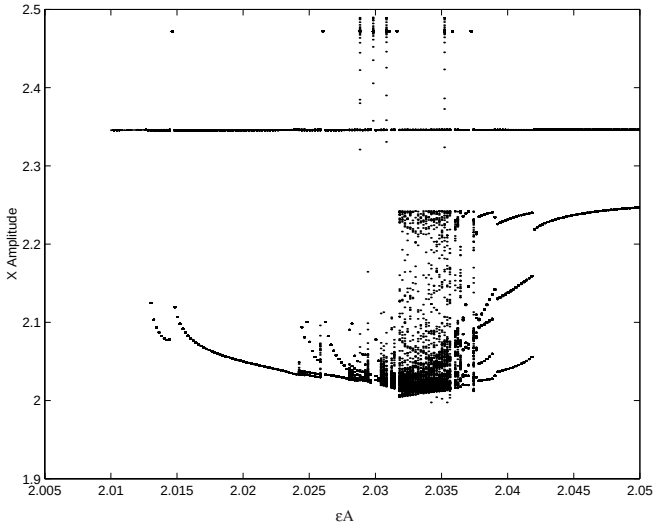

Figure 10: Bifurcation Plot, X Amplitude vs. εA (εB = -2.5).

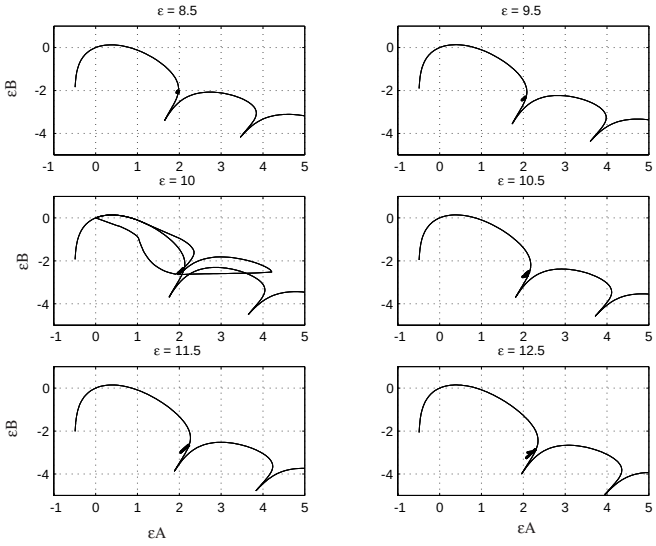

Figure 11: Chaos (shown in dark) on Transition Curves.

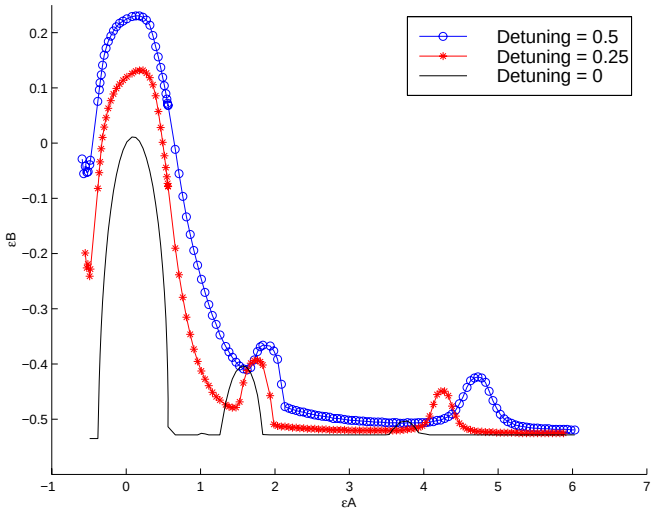

Figure 12: Transition Curves ($\varepsilon\Delta = 0.5$, $\varepsilon\Delta = 0.25$, $\varepsilon\Delta = 0$).

5 Detuning

The dynamic behaviors previously described were found in the system of two linearly coupled *identical* van der Pol oscillators. Thus, the detuning parameter, $\varepsilon\Delta$, was equal to zero throughout the numerical simulations keeping the natural frequencies of each oscillator identical. With both oscillators identical, their motion can be characterized as either unstable (εA < -0.5) or phase-locked (excluding the small areas of chaos) in one of the following modes: in-phase, out-of-phase, shifted symmetric or shifted asymmetric. When introducing detuning to the system ($\varepsilon\Delta \neq 0$), thus having two oscillators with different frequencies, new dynamic behavior has been discovered. This behavior will be discussed later.

Figure 12 shows the transition graphs for three different detuning values, ($\varepsilon\Delta = 0$, 0.25 and 0.5). As stated earlier, the curves represent the point at which the in-phase mode becomes unstable (above the curve, the in-phase mode is stable, below the curve the in-phase mode is unstable). All three transition curves have similar shapes; horizontal lines (B_{zmd}) along the εB axis with cascading ovals. It can be seen that as the detuning parameter increases the transition curve shifts up the εB axis (+ εB direction) and the ovals shift to the right on the εA axis (+ εA direction).

Figure 13 shows the transition curve for $\varepsilon\Delta = 0.25$ compared with the no-detuning case. The curve labeled in-phase (IP) shows where the in-phase mode loses stability (above the curve stable, below the curve unstable). The curve labeled out-of-phase (OOP) shows where both the in-phase mode and the no phase-locking mode lose stability (below the curve). For εA $\geq$ 0.5 both the in-phase curve and the out-of-phase curve are the same and the response of

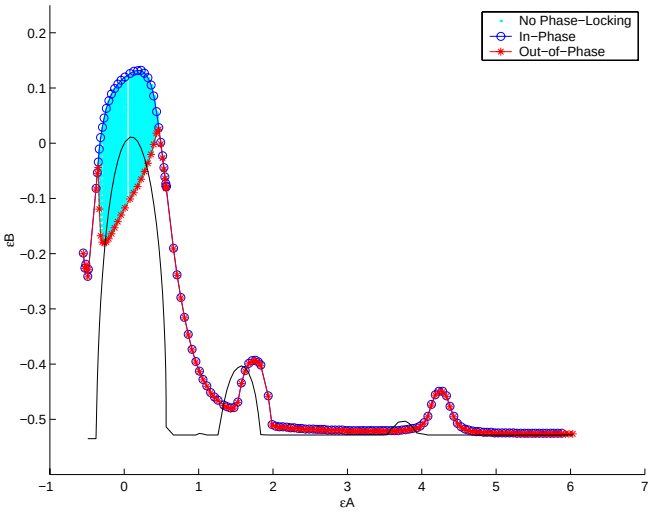

Figure 13: Transition Curve, ($\varepsilon\Delta = 0.25$ and $\varepsilon\Delta = 0$).

the oscillators is similar to the response of the oscillators without detuning, they transition from in-phase stability directly to out-of-phase stability. In the region bounded by -0.5 $\leq \varepsilon$A $\leq$ 0.5 the curves are different meaning there is no phase-locking mode found between the curves.

The expected behavior with no phase-locking is drift. Drift is found when the coupling parameters are small, thus each oscillator oscillates independently of the other with different frequencies. Quantitatively, drift is measured by calculating the phase lag (Eq. 4) between the oscillators. While drifting, the phase lag will grow. Conversely, phase-locked motion (in-phase, out-of-phase, shifted) has a constant phase lag. Figure 14 shows the time history of the drift found with $\varepsilon\Delta = 0.25$ and εA = εB = 0. The time history shows that each oscillator has a different frequency and the phase lag (time between zero crossings) is growing.

Figures 15 and 16 show time histories of the coupled oscillators within the region of no phase-locking. Each time history displays a much different behavior than the drift described earlier as each time history shows beating. Studying the response of Figure 15 one can see that the beating has a slower frequency than the response of Figure 16. One interesting note is the transition of the oscillators from the lowest amplitude back to the highest amplitude. In Figure 15 the frequency of the individual oscillators changes at this transition point while in Figure 16 the oscillator with the smallest amplitude (thick line) displays erratic behavior when transitioning to the higher amplitude. These different behaviors of the coupled oscillators are found on the edges of the no phase-locking regions very near the transition to the out-of-phase stability region.

The third dynamic behavior found in the no phase-locking region was chaos. Figure 17 shows the time history of the chaotic regime for $\varepsilon\Delta = 0.25$ with

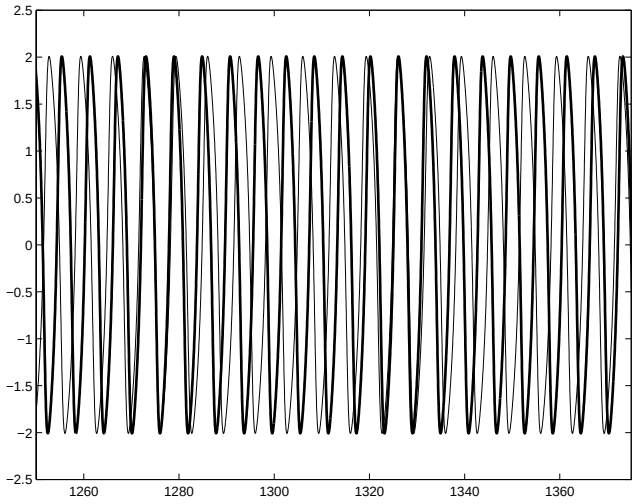

Figure 14: Time History, Drift, No Phase-Locking Region with Detuning, ($\varepsilon\Delta = 0.25$, $\varepsilon = 1$, εA = 0, εB = 0).

εA = -0.352 and εB = -0.043. Again, this behavior is found at the edge of the no phase-locking region near the transition point to out-of-phase stability.

Figure 18 shows the transition curve for $\varepsilon\Delta = 0.5$ compared with the no detuning case. The transition curves are similar to the transition curve for $\varepsilon\Delta = 0.25$, but with a larger no phase-locking region.

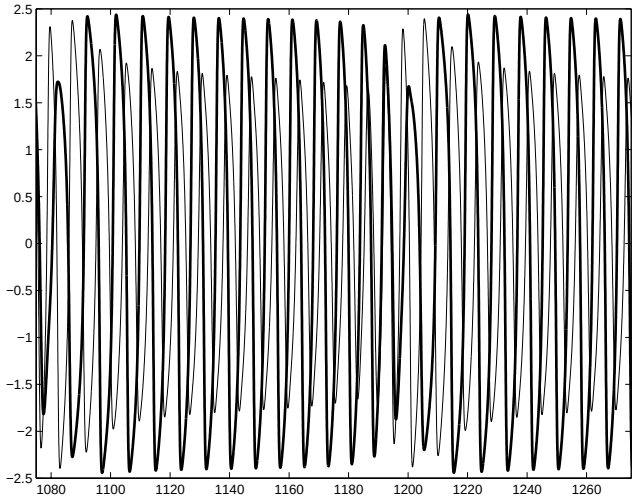

Figure 15: Time History, Beating, No Phase-Locking Region with Detuning, ($\varepsilon\Delta$ = 0.25, ε = 1, εA = -0.28, εB = -0.175).

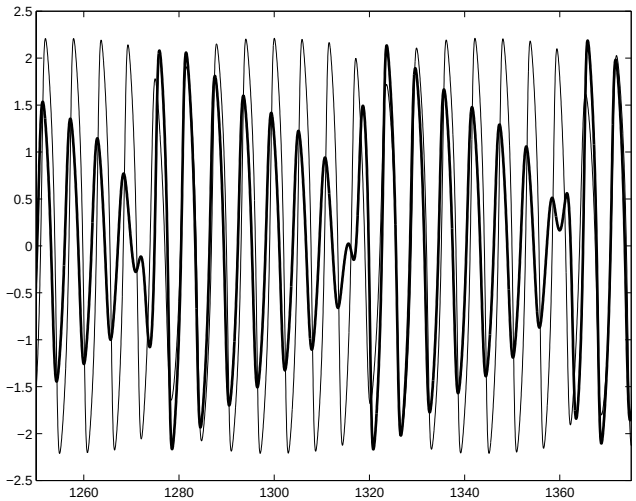

Figure 16: Time History, Beating, No Phase-Locking Region with Detuning, ($\varepsilon\Delta$ = 0.25, ε = 1, εA = 0.4912, εB = 0.0004).

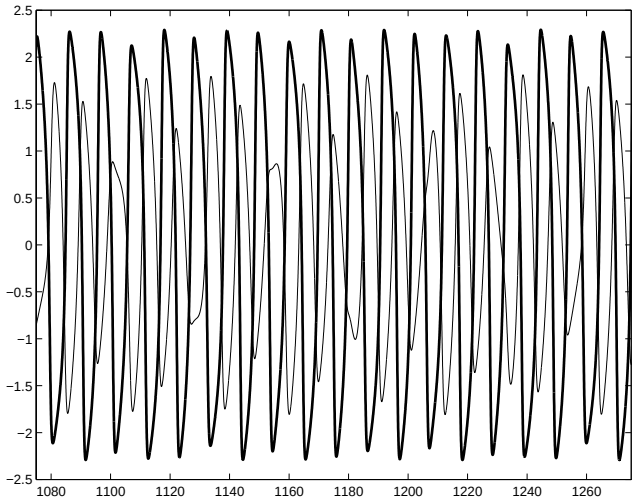

Figure 17: Time History, Chaos, No Phase-Locking Region with Detuning, ($\varepsilon\Delta$ = 0.25, ε = 1, εA = -0.352, εB = -0.043).

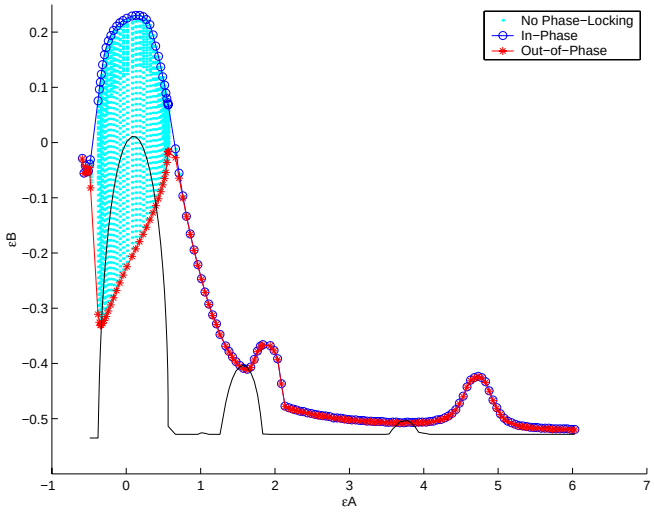

Figure 18: Transition Curve, ($\varepsilon\Delta$ = 0.5 and $\varepsilon\Delta$ = 0).

6 Conclusions

We have presented a complete description, using numerical simulations, of the dynamic behavior of a system of a pair of linearly coupled van der Pol oscillators. The different dynamic behaviors found include; shifted asymmetric, shifted symmetric and chaos. Time histories of each behavior has been presented in Figures 3, 4 and 8. Along with the actual time history of each behavior, the regions of each behavior has been mapped onto the coupling parameter space. These regions have also been described as the non-linearity parameter ε changes.

Also reported are the stability regions for the in-phase mode of a pair of coupled van der Pol oscillators with detuning. With small detuning added to one oscillator, the transition curves retain a similar shape as the transition curves without detuning; horizontal line (B_{zmd}) and cascading ovals. It was shown that as detuning increases the transition curve shifts up the εB axis. Therefore, as detuning increases the coupling parameters must be stronger in order for the in-phase mode to remain stable. Also reported were three dynamic behaviors found in the system with detuning; drift, beating and chaos.

References

[1] Alligood, K.T., Sauer, T.D. and Yorke, J.A., *Chaos An Introduction to Dynamical Systems.*

[2] Analog Devices, 1999, http://products.analog.com/ products/info.asp?product=AD534.

[3] Andersen, C.M., and Geer, J.F., 1982, Power Series Expansions for the Frequency and Period of the Limit Cycle of the van der Pol Equation, *SIAM Journal on Applied Mathematics*, 42, 678-693.

[4] Andronov, A.A. and Chaikin, C.E., 1949, *Theory of Oscillations.*

[5] Belair, J., 1984, 'Phase Locking in Linearly Coupled Relaxation Oscillators', Ph.D. Thesis, Cornell University, Ithaca, NY.

[6] Belair, J., and Holmes, P., 1984, On Linearly Coupled Relaxation Oscillators, *Q. Applied Mathematics*, 42, 193-219.

[7] Blevins, R.D., 1977, *Flow Induced Vibrations.*

[8] Carrier, G.F., 1953, Boundary Layer Problems in Applied Mathematics, *Advances in Applied Mechanics*, 3, 1-20.

[9] Chakraborty, T., and Rand, R.H., 1987, The transition from phase locking to drift in a system of two weakly coupled van der Pol oscillators, *International Journal of Non-Linear Mechanics*, 23, 369-376.

[10] Chen, L.Y., Goldenfeld, N., and Oono, Y., 1994, Renormalization Group Theory for Global Asymptotic Analysis, *Physics Review Letters*, 73(10), 1311-1314.

[11] Chen, S.S., 1987, *Flow Induced Vibration of Circular Cylindrical Structures.*

[12] Cohen, A.H., Holmes, P.J., and Rand, R.H., 1982, The nature of the coupling between segmental oscillators of the lamprey spinal generator for locomotion: A mathematical model, *Journal of Mathematical Biology*, 13, 345-369.

[13] Dadfar, M.B, Greer, J. and Andersen, C.M., 1984, Perturbation Analysis of the Limit Cycle of the van der Pol Equation, *SIAM Journal on Applied Mathematics*, 44, 881-895.

[14] Dorodnitsyn, A.A., 1947, Asymptotic Solution of the van der Pol Equation, *Proceedings of the Institute of Mechanics of the Academy of Science of the USSR*, XI

[15] Ermentrout, G.B., and Kopell, N., 1984, Frequency Plateaus in a Chain of Weakly Coupled Oscillators, *SIAM Journal of Mathematical Analysis*, 15, 215-237.

[16] Foo, S.Y., 1994, Coupled Nonlinear Oscillators in Biological Systems.

[17] Gillies, A.W., 1954, On the Transformations of Singularities and Limit Cycles of the Variational Equations of van der Pol, *Quarterly Journal of Mechanics and Applied Mathematics*, 7, 152-167.

[18] Glass, L. and Mackey, M.C., 1979, A Simple Model For Phase Locking of Biological Oscillators, *Journal of Mathematical Biology*, 7, 339-352.

[19] Grasman, J., 1987, *Asymptotic Methods for Relaxation Oscillations and Applications*.

[20] Grasman, J., Veling, E.J.M. and Willems, G.M., 1976, Relaxation Oscillations Governed by a van der Pol Equation, *SIAM Journal on Applied Mathematics*, 31, 667-676.

[21] Holmes, P.J., and Rand, D.A., 1978, Bifurcations of the Forced van der Pol Oscillators, *Quarterly of Applied Mathematics*, 35, 495-509.

[22] Izhikevich, E.M., 2000, Phase Equations for Relaxation Oscillators, *SIAM Journal on Applied Mathematics*, submitted.

[23] Jordan, D.W., and Smith, P., 1987, *Nonlinear Ordinary Differential Equations, 2^{nd} Ed.*

[24] Kaplan, D., and Glass, L., *Understanding Nonlinear Dynamics*.

[25] Keith, W.L., and Rand, R.H., 1984, 1:1 and 2:1 Phase Entrainment in a System of Two Coupled Limit Cycle Oscillators, *Journal of Mathematical Biology*, 20, 133-152.

[26] Keith, W.L., and Rand, R.H., 1985, Dynamics of a System Exhibiting the Global Bifurcation of a Limit Cycle at Infinity, *International Journal of Non-Linear Mechanics*, 20, 325-338.

[27] Kevorkian, J. and Cole, J.D., 1981, *Perturbation Methods in Applied Mathematics*.

[28] Kreyszig, E., 1993, *Advanced Engineering Mathematics*.

[29] LaSalle, J.P., 1949, Relaxation Oscillations, *Quarterly of Applied Mathematics*, 7.

[30] Levi, M., 1981, Qualitative Analysis of the Periodically Forced Relaxation Oscillations, *Memoirs of the American Mathematical Society*, 214, 1-147.

[31] Lotka, A.J., 1925, *Elements of Physical Biology*.

[32] Low, L.A., 1998, 'Stability Regions of Linearly Coupled van der Pol Oscillators', Master of Science Thesis, University of Washington, Seattle, Washington.

[33] Magnus, W., and Winkler, S., 1962, *Hill's Equation*.

[34] Minorsky, N.,1962, *Nonlinear Vibrations*.

[35] Motorola, 1999, http://mot-sps.com/sps/General/chips-nav.html.

[36] Moon, F.C., *Chaotic and Fractal Dynamics*.

[37] Mudavanhu, B., 2000, 'Singular Perturbation Techniques: The Multiple Scales, Averaging, Renormalization Group and Invariance-Condition Methods', University of Washington, Seattle, Washington.

[38] Mudavanhu, B., 2000, 'Stability Analysis of the Mathieu Equation Using Renormalization Group Method', University of Washington, Seattle, Washington.

[39] Murray, J.D.,1989, *Mathematical Biology*.

[40] National Semiconductor, 1999, http://www.national.com/pf/LM/LM323.html.

[41] Nayfeh, A., 1983, *Perturbation Methods*.

[42] Palm, E. and Tveitereid, M., 1980, On Coupled van der Pol Equations, *Quarterly Journal of Mechanics and Applied Mathematics*, 33, 267-276.

[43] Pavlidis, T., 1973, *Biological Oscillators: Their Mathematical Analysis*.

[44] Rand, R.H. and Armbruster, D., 1987, *Perturbation Methods, Bifurcation Theory and Computer Algebra.*

[45] Rand, R.H. and Ellison, J.L., 1986, Dynamics of Stomate Fields in Leaves, *Lectures on Mathematics in the Life Sciences*, 18, 51-86.

[46] Rand, R.H., and Holmes, P.J., 1980, Bifurcation of Periodic Motions in Two Weakly Coupled van der Pol Oscillators, *International Journal of Non-Linear Mechanics*, 15, 387-399.

[47] Rand, R.H., Storti, D.W., Upadhyaya, S.K., and Cooke, J.R., 1981, Dynamics of Coupled Stomatal Oscillators, *Journal of Mathematical Biology*, 15, 131-149.

[48] Reinhall, P.G. and Storti, D.W., 1995, A Numerical Investigation of Phase-Locked and Chaotic Behavior of Coupled van der Pol Oscillators, *Proceedings of the 15^{th} Biennial ASME Conference on Mechanical Vibration and Noise.*

[49] Rizzoni, G., 1993, *Principles and Applications of Electrical Engineering.*

[50] Sliger, D.M., 1997, 'Stability Transitions For Weakly Coupled Van Der Pol Oscillators', Master of Science Thesis, University of Washington, Seattle, Washington.

[51] Sprott, J.C., 1997, Chaos From Euler Solution of ODEs, *http://sprott.physics.wisc.edu/chaos/eulermap.htm*, University of Wisconsin, Madison, Wisconsin.

[52] Stoker, J.J., 1950, *Nonlinear Vibrations in Mechanical and Electrical Systems.*

[53] Storti, D.W., 1987, Bifurcations Which Destroy the Out-of-Phase Mode in a Pair of Linearly Coupled Relaxation Oscillators, *International Journal of Non-Linear Mechanics.*

[54] Storti, D.W., Nevrinceanu, C., and Reinhall, P.G., 1993, Perturbation Solution of an Oscillator with Periodic van der Pol Damping, *Dynamics and Vibration of Time-Varying Systems and Structures, ASME DE*, 56, 397-402.

[55] Storti, D.W. and Rand, R.H., 1982, Dynamics of Two Strongly Coupled van der Pol Oscillators, *International Journal of Non-Linear Mechanics*, 17, 143-152.

[56] Storti, D.W., and Rand, R.H., 1986, Dynamics of Two Strongly Coupled van der Pol Oscillators, *SIAM Journal on Applied Mathematics*, 46, 56-67.

[57] Storti, D.W., and Reinhall, P.G., 1993, *Stability of In-Phase and Out-of-Phase Modes for Coupled van der Pol Oscillators.*

[58] Storti, D.W., and Reinhall, P.G., 1996, *Hill's Equation Analysis of Phase-Locked Mode Stability for Coupled van der Pol Oscillators.*

[59] Storti, D.W., and Reinhall, P.G., 1999, *Phase-Locked Mode Stability For Coupled van der Pol Oscillators.*

[60] Ünsal, C., 1993, 'Self Organization in Large Populations of Mobile Robots', Master of Science Thesis, Virginia Polytechnic Institute and State University, Blacksburg, Virginia.

[61] van der Pol, B., 1926, On Relaxation Oscillations, *Philosophical Magazine*, 7, 978-992.

[62] van der Pol, B., 1927, Forced Oscillations in a Circuit with Nonlinear Resistance (Receptance with Reactive Triode), *Selected Papers on Mathematical Trends in Control Theory*, Bellman and Kalaba, Editors.

[63] van der Pol, B., and van der Mark, J., 1928, The Heartbeat Considered as a Relaxation Oscillation, and an Electrical Model of the Heart, *Philosophical Magazine*, 7, 763-775.